

Transition from a Spin Luttinger–Liquid to a Bose–Einstein Condensate of Magnons in the Quantum Spin Ladder $(\text{C}_5\text{H}_{12}\text{N})_2\text{CuBr}_4$

B. Thielemann,¹ Ch. Rüegg,² K. Kiefer,³ H. M. Rønnow,⁴ P. Bouillot,⁵ C. Kollath,⁶ E. Orignac,⁷ R. Citro,⁸ T. Giamarchi,⁵ A. M. Läuchli,⁹ D. Biner,¹⁰ K. Krämer,¹⁰ F. Wolff–Fabris,¹¹ V. Zapf,¹¹ M. Jaime,¹¹ J. Stahn,¹ N.B. Christensen,^{1,12} B. Grenier,¹³ D. F. McMorrow,² and J. Mesot^{1,4}

¹Laboratory for Neutron Scattering, ETH Zurich and Paul Scherrer Institute, CH–5232 Villigen, Switzerland

²London Centre for Nanotechnology, University College London, London WC1E 6BT, United Kingdom

³BENSC, Helmholtz Centre Berlin for Materials and Energy, D–14109 Berlin, Germany

⁴Laboratory for Quantum Magnetism, Ecole Polytechnique Fédérale de Lausanne, CH–1015 Lausanne, Switzerland

⁵DPMC–MaNEP, University of Geneva, CH–1211 Geneva, Switzerland

⁶Centre de Physique Théorique, Ecole Polytechnique, CNRS, 91128 Palaiseau Cedex, France

⁷LPENSL CNRS UMR 5672, F–69364 Lyon Cedex 07, France

⁸Dipartimento di Fisica “E. R. Caianiello” and CNISM, Università di Salerno, I–84100 Salerno, Italy

⁹Institut Romand de Recherche Numérique en Physique des Matériaux (IRRMA), CH–1015 Lausanne, Switzerland

¹⁰Department for Chemistry and Biochemistry, University of Bern, CH–3000 Bern 9, Switzerland

¹¹MPA–NHMFL, Los Alamos National Laboratory, Los Alamos, New Mexico 87545, USA

¹²Risø National Laboratory for Sust. Energy, Technical University of Denmark, DK–4000 Roskilde

¹³Université Joseph Fourier, Grenoble and CEA–Grenoble, INAC/SPSMS/MDN, F–38054 Grenoble, France

(Dated: April 15, 2022)

The transition from a magnetic field–tuned spin Luttinger–liquid with algebraic spin correlations to a Bose–Einstein Condensate of magnons with long–range magnetic order is investigated in the two–leg spin ladder material bis(piperidinium)tetrabromocuprate(II) $(\text{C}_5\text{H}_{12}\text{N})_2\text{CuBr}_4$. By neutron diffraction and measurements of the magnetocaloric effect we show that the ordering temperature, transverse and longitudinal magnetizations, and critical behavior are highly dominated by the tunable one–dimensional physics of the weakly–coupled spin Luttinger–liquids. Our experimental results are in excellent agreement with theoretical calculations with renormalized mean–field interaction parameters.

PACS numbers: 75.10.Jm; 75.30.Kz; 75.25.+z; 75.40.Mg

Low–dimensional magnets have been the subject of intense research for decades. Examples include studies of one–dimensional (1D) chains and ladders and their intriguing ground and excited state properties [1, 2, 3, 4, 5, 6, 7]. In this context residual interactions between the low–dimensional units, which are always present in real materials, might at first sight be viewed as a distraction from the physics of interest. On the other hand such interactions allow investigations of a number of fascinating questions regarding the crossover from 1D to 3D behavior. For example in 3D, magnons in a gapped magnet undergo Bose–Einstein Condensation (BEC) at a magnetic field H_c , where the gap is closed by the Zeeman effect ([8] and references therein). At this quantum critical point (QCP), the spin components perpendicular to the magnetic field develop long–range antiferromagnetic (AF) order of 3D–XY type. In contrast in 1D, quantum phase fluctuations destroy any long–range order and a critical phase with algebraic spin correlations – a spin Luttinger–liquid (LL) – is predicted by theory [4, 7]. While the spin LL may also be realized in coupled $S = 1/2$ chains, e.g. in KCuF_3 [9, 10], a particularly rich phase diagram including a transition between the spin LL and an ordered phase is expected for the quasi–1D case of weakly coupled ladders [7]. Interestingly, the LL parameters can be tuned directly by a magnetic field.

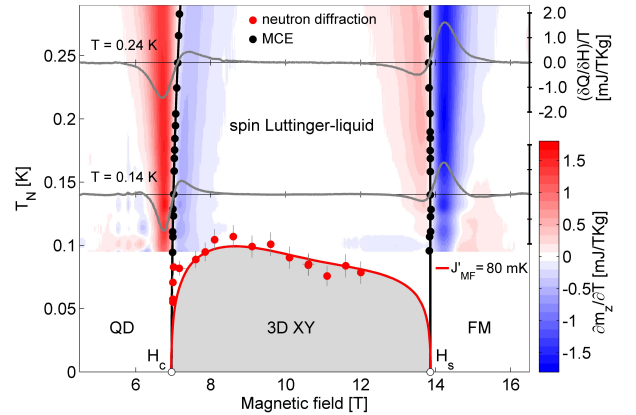


FIG. 1: Low temperature phase diagram of $(\text{C}_5\text{H}_{12}\text{N})_2\text{CuBr}_4$. The crossover temperature to the spin LL and phase transition to the BEC with 3D–XY magnetic order are presented as derived from measurements of the MCE and neutron diffraction, respectively. The contour plot is based on 18 individual field scans of the MCE (two shown as gray lines), using $(\delta Q/\delta H)/T = -(\partial m_z/\partial T)$ [18]. The spin LL extends up to 1.5 K at $H = (H_c + H_s)/2$.

In this Letter we report the results of a comprehensive neutron diffraction study combined with measurements

of the magnetocaloric effect (MCE) of the two-leg ladder material $(\text{C}_5\text{H}_{12}\text{N})_2\text{CuBr}_4$. A transition at dilution temperatures between a field-tuned LL phase and an ordered AF phase, as summarized in Fig. 1, occurs when the coupled spin LLs are cooled to temperatures of the order of the interladder interactions. However, the ordered phase remains highly dominated by the LL physics of the low-dimensional subunits, through the LL exponent K and the spin-wave velocity u . We find a characteristic field dependence of the ordering temperature $T_N(H)$ on these LL parameters and determine the spin structure as well as the transverse and longitudinal magnetic moment. These results allow a quantitative test of recent calculations by bosonization and density-matrix renormalization group (DMRG, [11]), as well as Quantum Monte-Carlo (QMC) for interacting ladders.

Materials realizing 1D spin ladders with critical fields H_c and H_s (magnetic saturation, FM) accessible in the laboratory are rare [3], or often have additional terms in the Hamiltonian, such that an interpretation in the framework of a spin LL becomes inappropriate, e.g. CuHpCl [12, 13, 14]. The compound $(\text{C}_5\text{H}_{12}\text{N})_2\text{CuBr}_4$ is an exception [11, 15, 16, 17, 18]. Its low-temperature specific heat is in quantitative agreement with ladder predictions [18] and inelastic neutron scattering (INS) demonstrates its excellent low-dimensionality [19]. The gapped triplet excitations in zero-field are in good agreement with calculations based on second-order perturbation theory and a ladder Hamiltonian with rung and leg exchange $J_r = 12.9(1)$ K and $J_l = 3.3(1)$ K, respectively.

High quality single crystals of $(\text{C}_5\text{H}_{12}\text{N})_2\text{CuBr}_4$ (abbr. Hpip) and $(\text{C}_5\text{D}_{12}\text{N})_2\text{CuBr}_4$ (abbr. Dpip) were grown from solution. The MCE was measured on single crystalline Hpip in a standard dilution refrigerator at the NMFLL Los Alamos with sweep rates between 0.025 T/min and 0.075 T/min. Neutron diffraction experiments were performed on Dpip single crystals with sample mass 200 mg on the instruments D23 (ILL) and RITA-2 (SINQ/PSI), using standard diffraction setups. For all measurements a vertical magnetic field was applied along the crystallographic b -axis, perpendicular to the ladders that run along the a -axis.

As detailed in [18], the MCE provides a method to map the crossover from the gapped quantum-disordered (QD) regime of the spin ladder into the spin LL, which is marked by local extrema in the temperature dependence of the longitudinal magnetization ($\partial m_z / \partial T = 0$). The contour plot in Fig. 1 shows $\partial m_z / \partial T$ down to 100 mK. The phase boundary data (black circles in Fig. 1) are analyzed by a sliding window technique [20, 21]. In a first step, the critical fields are determined to be $H_c = 6.96(2)$ T and $H_s = 13.85(3)$ T. Subsequently the critical fields are fixed to those values and a fit to $T_{LL} \propto (H - H_c)^{\frac{1}{\nu}}$ yields an exponent $\nu = 2.1(1)$ at H_c in the window for the lowest measured temperatures (0.1-

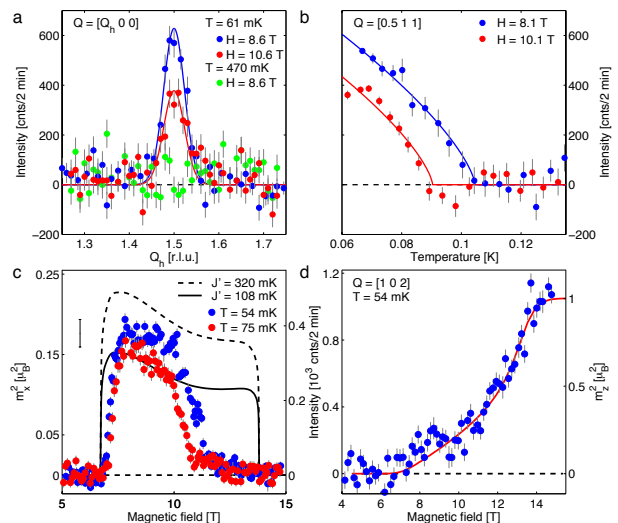


FIG. 2: Summary of neutron diffraction data. (a) Q -scans across an AF Bragg peak after subtraction of the flat background at $H = 6$ T and $T = 63$ mK (QD phase). (b) T -dependence of the Bragg intensity demonstrating the onset of 3D long-range order at $T_N(H)$, solid lines are fits to the 3D-XY model. (c) H -dependence of the square of the transverse moment m_x^2 measured at $Q = (1.5 0 0)$ for $T = 54$ mK (blue) and $T = 75$ mK (red). The solid and dashed line are from DMRG calculations for interladder interactions J' as defined. Error bars on data points are based on counting statistics. The vertical black line indicates the systematic error of the calibration to absolute units. (d) Magnetic signal at $Q = (1 0 2)$ which is proportional to the square of the uniform magnetisation m_z^2 . Neutron intensity after subtraction of the nuclear contribution which also corrects for magnetostriction. The red line is a fit to a QMC calculation.

0.15 K) [22]. For a ladder in a field, $\nu = 1$ is predicted by theory [5] since close to H_c the spin system maps onto a free fermion model (LL exponent $K = 1$). However, as can be seen from our DMRG determination of $K(H)$ [11], K decreases rapidly in the vicinity of H_c and H_s . Consequently the true critical regime is very narrow, which is in agreement with QMC calculations for the related Haldane spin chains [23]. The present MCE results extend our previous measurements [18] to temperatures below 300 mK and demonstrate spin LL behavior down to 100 mK. We find an upper limit for the universal regime in quantum spin ladders of $T/J_l \approx 0.03$.

In Fig. 2 we summarize our neutron diffraction data. Fig. 2(a) shows Q -scans across the AF position $Q = (1.5 0 0)$ when cooling the sample from the spin LL at $H_c < H < H_s$. Resolution-limited magnetic Bragg peaks are observed at base temperature, demonstrating long-range AF order. The peak is absent in a scan at $T = 470$ mK and $H = 8.6$ T in the spin LL. The magnetic Bragg intensity decreases with increasing magnetic field, indicating a substantial field dependence of the transverse ordered moment. In Fig. 2(b) the temperature de-

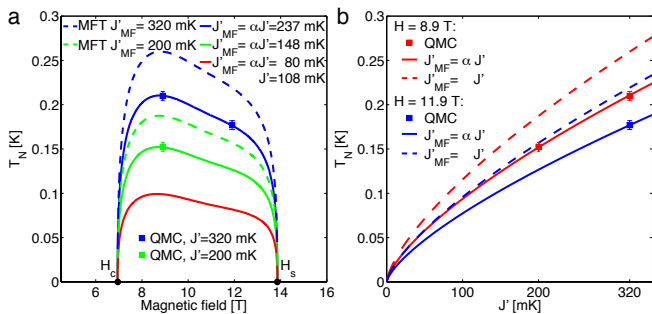


FIG. 3: The 3D-XY phase boundary by DMRG mean-field theory (MFT) and QMC. (a) $T_N(H)$ for several values of J' , as indicated, $\alpha = 0.74(1)$. (b) T_N as a function of J' .

pendence of the Bragg peak intensity is presented which is used for the determination of the 3D-XY phase boundary (red circles in Fig. 1). We note that $T_N(H)$ has a maximum away from $m_z = 1/2$, which is in agreement with recent NMR results [11], but in strong contrast to spin systems in higher dimensions, e.g. $\text{BaCuSi}_2\text{O}_6$ [21]. The observed asymmetry comes from the moderate coupling ratio J_r/J_l for which all four states of the ladder must be retained, breaking particle-hole symmetry between H_c and H_s . Such asymmetry is apparent in QMC studies of coupled ladders [24]. Here we use bosonization, DMRG and a mean-field treatment of the interladder interactions, as detailed in Ref. [11], to model our experimental data for $T_N(H)$ (red line in Fig. 1). In this approach $T_N(H)$ depends on the LL exponent $K(H)$, spin wave velocity $u(H)$, and correlation amplitude $A_x(H)$, which are obtained from DMRG and bosonization for a ladder with coupling ratio 3.6. The only free parameter is the mean-field interladder exchange J'_{MF} [Fig. 3]. The solid red line in Fig. 1 is a fit to the experimental data that yields $J'_{MF} = 80(5)$ mK [25], consistent with the value reported in Ref. [11].

However, to obtain the bare value of J' it is necessary to correct for the (interladder) mean-field approximation that underestimates fluctuations and thus J' for a given T_c . For coupled 1D chains, mean-field overestimates T_N by approximately 50% [9]. As shown numerically quantitative agreement can be recovered by introducing a renormalization factor α multiplying the coordination number z of the coupled 1D system, $J'_{MF} = \alpha J' = \alpha z \tilde{J}'$, where \tilde{J}' is the microscopic exchange between magnetic ions [26]. To determine α for the case of coupled 1D ladders, some information about z and \tilde{J}' is needed. INS measurements, of the very small triplet dispersion along the b and c axes demonstrate that in a minimal model one additional interladder interaction is relevant, $\tilde{J}' = J_3$, which connects, in the notation of Ref. [27], ladders of different orientation along the $(1\ 0.5\ 0.5)$ direction with four nearest neighbors, $z = 4$ [Fig. 4]. Details on the

results, spin dynamics and exchange paths will be presented elsewhere [19]. Using this interladder exchange geometry, we performed QMC simulations [28, 29] of the 3D ordering temperature at $H = 8.9$ T and 11.9 T for two values of J' [Fig. 3(a)]. For $\alpha = 0.74(1)$, which is similar to the value obtained for the coupled chains [26], we find perfect agreement between the mean-field treatment of the interladder exchange and QMC, as shown in Fig. 3(b). Hence the best mean-field fit $J'_{MF} = 80(5)$ mK in Fig. 1 corresponds to a true (microscopic) $J' = 108(7)$ mK and thus $\tilde{J}' = 27(2)$ mK per coupling [30].

Neutron diffraction also allows the magnetic structure, the uniform longitudinal (m_z) and staggered transverse (m_x) magnetization to be determined quantitatively. At base temperature and $H = 8.6$ T (maximum $T_N \approx 110$ mK) the intensities of a total of 26 AF Bragg peaks were recorded on D23. Amongst four magnetic structures allowed by group theory, the one with the spins aligned perpendicular to the a -axis and antiparallel within the ladder and with respect to the adjacent ladders (propagation vector $k = (0.5\ 0\ 0)$, Fig. 4) provides the best fit ($\chi^2 = 5.54$). This information implies further constraints on the interladder exchange, and is consistent with the expected sign of \tilde{J}' . The ordered moment is $0.41(2) \mu_B$ per copper ion. The alignment perpendicular to the a -axis shows additionally that the transverse component of the spins is parallel to the maximum of the g -factor in the ac -plane [15].

Once the spin gap is closed, the triplet density in the ground state becomes finite and the uniform magnetization m_z increases monotonically, which generates a ferromagnetic signal on top of nuclear Bragg peaks. A field scan of the magnetic intensity at $Q = (1\ 0\ 2)$ is presented

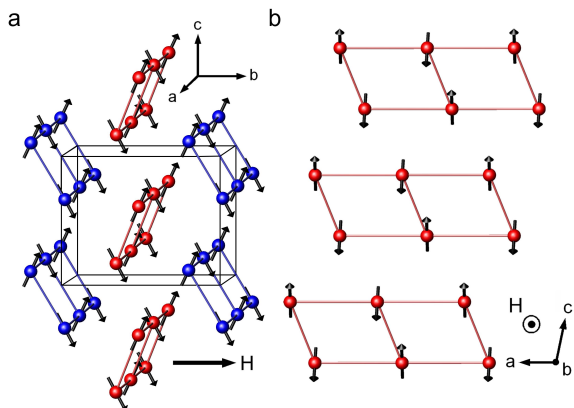


FIG. 4: Magnetic structure of $(\text{C}_5\text{H}_{12}\text{N})_2\text{CuBr}_4$. Only the copper atoms forming the ladder are shown (red/blue). Spin structure (black arrows) in the 3D ordered phase as determined by neutron diffraction at $H = 8.6$ T and $T = 63$ mK. The spin component along the field ($H||b$) is fixed to the value obtained from QMC calculations. Projection on the bc -plane in (a) and on the ac -plane in (b).

in Fig. 2 (d). The red line is a fit to a QMC calculation of the ladder magnetization m_z^2 with exchange interactions from INS. Given the weak magnetic signal competing with the strong nuclear peak, the overall agreement is reasonable, in particular at high magnetic fields around H_s where the magnetic intensity is also high. Fig. 2 (c) shows field scans of the AF Bragg intensity at $Q = (1.5 \ 0 \ 0)$ for $T = 54$ mK and $T = 75$ mK. The observed intensity is proportional to the square of the transverse magnetization m_x^2 and was scaled to the ordered moment determined at $H = 8.6$ T from the complete refinement of the spin structure (above). In contrast to e.g. NMR, m_x^2 can be determined quantitatively by neutron scattering, allowing additional tests of theoretical predictions. The temperature dependence of $m_x(T)^2$ in Fig. 2 (b) indicates clearly that the AF order parameter is not completely saturated at the base temperature of our experimental setup and due to the same limitation, the AF transition (and corresponding Bragg peak intensity) cannot be observed for $H > 12$ T. Hence the measured transverse moment is expected to be smaller than the saturated value at $T = 0$ K and suppressed at high fields. The comparison between the experimental data and the DMRG calculations (black lines, $T = 0$ K) is consistent with this expectation. We use again $J' = 108$ mK (best fit to the phase boundary) and $J' = 320$ mK. The former value still slightly underestimates the transverse moment, but gives reasonable agreement with the data. As for the phase boundary, m_x is clearly dominated by the 1D LL physics, though it originates from 3D interactions. Its asymmetry is again explained by the field-dependence of the LL parameters and H_{pip} being not entirely in the strong-coupling limit.

In summary, comprehensive neutron diffraction data and measurements of the magnetocaloric effect are presented of the transition between 1D and 3D physics in coupled spin Luttinger-liquids, realized in the exceptional spin ladder material $(\text{C}_5\text{H}_{12}\text{N})_2\text{CuBr}_4$ in a magnetic field. This compound has an optimal separation of energy scales of magnetic exchange interactions to allow such an investigation, and comparison with detailed predictions by theory. We find that the properties of the BEC phase with 3D long-range magnetic order, occurring at temperatures of the order of the interladder exchange, are dominated by the Luttinger-liquid parameters of the isolated ladders, and hence can be tuned continuously by the magnetic field. The unconventional field-dependence of the Néel temperature and the transverse magnetization are in good agreement with DMRG calculations and a mean-field treatment of the (renormalized) interladder interactions. By comparison with QMC simulations we determine the renormalization factor for coupled ladders.

We thank C. Berthier and B. Normand for insightful discussions. This project was supported by the Swiss National Science Foundation through NCCR MaNEP

and Division II, Royal Society, EPSRC, NSF, DOE, the RTRA network "Triangle de la Physique", and the State of Florida through the National High Magnetic Field Laboratory. This work is partially based on experiments performed at the Swiss spallation neutron source SINQ, Paul Scherrer Institute, Villigen, Switzerland.

-
- [1] H. Bethe, Z. Phys. **71**, 205 (1931).
 - [2] F. D. M. Haldane, Phys. Lett. **93**, 464 (1983).
 - [3] E. Dagotto and T. M. Rice, Science **271**, 618 (1996).
 - [4] S. Sachdev, T. Senthil, and R. Shankar, Phys. Rev. B **50**, 258 (1994).
 - [5] R. Chitra and T. Giamarchi, Phys. Rev. B **55**, 5816 (1997).
 - [6] A. Furusaki and S. C. Zhang, Phys. Rev. B **60**, 1175 (1999).
 - [7] T. Giamarchi and A. M. Tsvelik, Phys. Rev. B **59**, 11398 (1999).
 - [8] T. Giamarchi, Ch. Rüegg, and O. Tchernyshyov, Nature Physics **4**, 198 (2008).
 - [9] H. J. Schulz, Phys. Rev. Lett. **77**, 2790 (1996)
 - [10] B. Lake, D. A. Tennant, C. D. Frost, and S. E. Nagler, Nature Materials **4**, 329 (2005).
 - [11] M. Klanjsek *et al.*, arXiv:0804.2639v2.
 - [12] G. Chaboussant *et al.*, Eur. Phys. J. B **6**, 167 (1998).
 - [13] M.B. Stone *et al.*, Phys. Rev. B **65**, 064423 (2002).
 - [14] M. Clémancey *et al.*, Phys. Rev. Lett. **97**, 167204 (2006).
 - [15] B.R. Patyal, B.L. Scott, and R.D. Willett, Phys. Rev. B **41**, 1657 (1990).
 - [16] B.C. Watson *et al.*, Phys. Rev. Lett. **86**, 5168 (2001).
 - [17] T. Lorenz *et al.*, Phys. Rev. Lett. **100**, 067208 (2008).
 - [18] Ch. Rüegg *et al.*, arXiv:0808.2715v1.
 - [19] B. Thielemann *et al.*, (to be published).
 - [20] O. Nohadani, S. Wessel, B. Normand, and S. Haas, Phys. Rev. B **69**, 220402 (2004).
 - [21] S. E. Sebastian *et al.*, Nature **441**, 617 (2006).
 - [22] At H_s the exponent ν cannot be determined quantitatively (line in Fig. 1 is for $\nu = 2$). Contributions from the Shottky anomaly of the nuclear spins to the heat capacity are important [18] and lead to long relaxation times.
 - [23] Y. Maeda, C. Hotta, and M. Oshikawa, Phys. Rev. Lett. **99**, 057205 (2007).
 - [24] S. Wessel, M. Olshanii, and S. Haas, Phys. Rev. Lett. **87**, 206407 (2001).
 - [25] Compared to the notation of [11] the coordination number $z = 4$ is included here in J'_{MF} .
 - [26] C. Yasuda *et al.*, Phys. Rev. Lett. **94**, 217201 (2005).
 - [27] M. Matsumoto, B. Normand, T. M. Rice, and M. Sigrist, Phys. Rev. B **69**, 054423 (2004).
 - [28] A.F. Albuquerque *et al.*, J. Magn. Magn. Mat. **310**, 1187 (2007).
 - [29] F. Alet *et al.*, Phys. Rev. E **71**, 36707, (2005).
 - [30] We note that $J_3 = 0.08(3)$ K, as experimentally determined by INS [19], is higher than what is found here from systematic fits to the phase boundary, $J_3 = 0.027(2)$ K. However, additional, e.g. ferromagnetic, interladder exchange of the order of 0.04 K can not be excluded due to limited INS resolution. Hence, both determinations may be consistent within error.